Radiological Physics and Technology (2022) 15:135–146
https://doi.org/10.1007/s12194-022-00655-5

RESEARCH ARTICLE

The impact of target positioning error and tumor size on radiobiological parameters in robotic stereotactic radiosurgery for metastatic brain tumors

Takeshi Takizawa[1,2] · Satoshi Tanabe[3] · Hisashi Nakano[3] · Satoru Utsunomiya[4] · Madoka Sakai[3] · Katsuya Maruyama[1] · Shigekazu Takeuchi[5] · Toshimichi Nakano[2] · Atsushi Ohta[3] · Motoki Kaidu[2] · Hiroyuki Ishikawa[2] · Kiyoshi Onda[5]

Received: 4 October 2021 / Revised: 25 February 2022 / Accepted: 26 February 2022 / Published online: 7 March 2022

Abstract

This study aimed to evaluate the effect of target positioning error (TPE) on radiobiological parameters, such as tumor control probability (TCP) and normal tissue complication probability (NTCP), in stereotactic radiosurgery (SRS) for metastatic brain tumors of different sizes using CyberKnife. The reference SRS plans were created using the circular cone of the CyberKnife for each spherical gross tumor volume (GTV) with diameters (φ) of 5, 7.5, 10, 15, and 20 mm, contoured on computed tomography images of the head phantom. Subsequently, plans involving TPE were created by shifting the beam center by 0.1–2.0 mm in three dimensions relative to the reference plans using the same beam arrangements. Conformity index (CI), generalized equivalent uniform dose (gEUD)-based TCP, and NTCP of estimated brain necrosis were evaluated for each plan. When the gEUD parameter "a" was set to − 10, the CI and TCP for the reference plan at the φ5-mm GTV were 0.90 and 80.8%, respectively. The corresponding values for plans involving TPE of 0.5-mm, 1.0-mm, and 2.0-mm were 0.62 and 77.4%, 0.40 and 62.9%, and 0.12 and 7.2%, respectively. In contrast, the NTCP for all GTVs were the same. The TCP for the plans involving a TPE of 2-mm was 7.2% and 68.8% at the φ5-mm and φ20-mm GTV, respectively. The TPEs corresponding to a TCP reduction rate of 3% at the φ5-mm and φ20-mm GTV were 0.41 and 0.99 mm, respectively. TPE had a significant effect on TCP in SRS for metastatic brain tumors using CyberKnife, particularly for small GTVs.

Keywords Stereotactic radiosurgery · CyberKnife · Dosimetric comparison · Tumor control probability · Normal tissue complication probability · Target positioning error

1 Introduction

Brain metastasis occurs in 20–40% of patients with cancer [1]. Stereotactic radiosurgery (SRS) is a single-high-dose irradiation technique that offers high geometric accuracy and aims to maximize tumor control probability (TCP) while minimizing normal tissue complication probability (NTCP) [1–3]. Equipment such as a linear accelerator (LINAC), Gamma Knife, and CyberKnife have been used for SRS [1, 4]. There are 356 CyberKnife units in operation worldwide and 40 units in Japan as of 2021 [5]. CyberKnife offers high mechanical accuracy and is equipped with a 6D skull tracking system, helping to achieve high target positioning accuracy [6]. In addition, CyberKnife can deliver a high degree of freedom and achieve high-dose conformity to the target volume [7, 8]. In SRS for metastatic brain tumors, CyberKnife-based plans have a steeper dose gradient around

✉ Takeshi Takizawa
takizawa@niigata-nogeka.or.jp

1 Department of Radiation Oncology, Niigata Neurosurgical Hospital, 3057 Yamada, Nishi-ku, Niigata 950-1101, Japan

2 Department of Radiology and Radiation Oncology, Niigata University Graduate School of Medical and Dental Sciences, 1-757 Asahimachi-dori, Chuo-ku, Niigata 951-8510, Japan

3 Department of Radiation Oncology, Niigata University Medical and Dental Hospital, 1-757 Asahimachi-dori, Chuo-ku, Niigata 951-8510, Japan

4 Department of Radiological Technology, Niigata University Graduate School of Health Sciences, 2-746 Asahimachi-dori, Chuo-ku, Niigata 951-8518, Japan

5 Department of Neurosurgery, Niigata Neurosurgical Hospital, 3057 Yamada, Nishi-ku, Niigata 950-1101, Japan

the tumor than LINAC-based plans and are superior in terms of reducing the dose to normal organs. [9, 10]

TCP and NTCP are clinically important outcome indicators in patients with brain metastasis undergoing SRS. TCP is estimated based on the relationship between the prescribed dose and 12-month local control rate, whereas NTCP is estimated based on the relationship between the incidence of brain necrosis and the volume of the brain receiving 14 Gy (V_{14}) [1, 11–13].

Target positioning accuracy is paramount in SRS because of the steep dose gradient around the target [14]. In general, a geometric positioning accuracy of 1 mm is required for SRS [14, 15], and a report from the American Association of Physicists in Medicine task group 135 (AAPM TG135) stipulates that CyberKnife should have a geometric positioning accuracy of < 0.95 mm [16]. However, there are concerns regarding the feasibility of a geometric accuracy of 1 mm in all cases. Importantly, tumor size was not considered when setting these reference values [14–16]. Even with the same positioning error, a reduction in tumor size may lead to a reduction in target dose coverage. Several reports on LINAC-based stereotactic radiotherapy have shown that positioning errors of a few millimeters could have a large impact on the reduction of the target dose [17–19]. Winey et al. assessed the impact of geometric uncertainty on dose distribution in LINAC-based plans for the treatment of multiple non-isocentric intracranial lesions. They reported that a 2-mm error led to a 43% reduction in the volume receiving the prescribed dose for a 6-mm tumor [18].

In addition, the above-mentioned studies focused only on changes in dose distribution. To estimate the clinical outcomes at the time of treatment planning, it is desirable to evaluate radiobiological parameters such as TCP and NTCP. Therefore, it is clinically important to evaluate the impact of the target positioning accuracy and tumor size on TCP and NTCP. Kraft et al. reported the clinical outcome of multiple brain metastases focused on the dependence of distance to the isocenter, and concluded that the distance to the isocenter does not affect the clinical outcome of SRS/stereotactic radiotherapy (SRT) [20]. They also concluded that the high positioning accuracy of ExacTrac maintained its clinical outcome. However, there is no detailed information regarding actual positioning accuracy. Therefore, it would be useful for many institutions to assess the impact of positioning accuracy on clinical outcomes from a physical perspective using a radiobiological model. Regarding the relationship between the target positioning accuracy and TCP, Nakano et al. investigated the effect of a setup error on TCP in simulation-based single-isocenter SRS for multiple brain metastases and found that a setup error of a few millimeters could significantly reduce the dose coverage and TCP for a small tumor [19, 21]. However, to the best of our knowledge, no studies have directly evaluated the relationship between target positioning accuracy and TCP/NTCP for each tumor size using conventional LINAC, Gamma Knife, or CyberKnife. In particular, there is concern that the CyberKnife-based SRS plan has a steeper dose gradient around the tumor, which may accentuate the effect of positioning errors. This study aimed to evaluate the effect of target positioning accuracy on dose distributions, TCP, NTCP, and tumor size in SRS using CyberKnife for metastatic brain tumors of five different sizes. To the best of our knowledge, this is the first study to assess the impact of target positioning accuracy on tumor size, physical dose distribution, and radiobiological parameters associated with patient outcomes in SRS for metastatic brain tumors using CyberKnife.

2 Materials and methods

In this study, an anthropomorphic head and neck phantom (Accuray, Sunnyvale, CA, USA) was used to simulate SRS plans for metastatic brain tumors. Thin-sliced high-resolution computed tomography (CT) images were obtained using a 320-slice CT scanner (Aquilion One, Canon Medical Systems, Tochigi, Japan) under the following conditions: 250-mm field of view, 512 × 512 matrix size, and 0.5-mm slice thickness (0.5-mm voxel size). To simulate metastatic brain tumors, virtual gross tumor volumes (GTVs) were contoured at the center of the brain on CT scans of the head phantom, which was defined as the volume of a sphere with a diameter (φ) of 5, 7.5, 10, 15, or 20 mm. In previous studies, the GTV-to-planning target volume (PTV) margin was set to 0 mm to minimize the NTCP of brain necrosis [14, 22, 23].

Consequently, the GTV-to-PTV margin in this study was set to 0 mm. The brain volume was contoured as an organ at risk. All treatment plans were generated using the Precision treatment planning system version 2.0.0.1 (Accuray, Sunnyvale, CA, USA). In this study, a 6-MV flattening filter-free photon beam was used. The beam size was controlled using a fixed circular collimator in the CyberKnife M6 series (Accuray, Sunnyvale, CA, USA), and φ of the collimator was selected to be the same size as the GTV ($\varphi = 5$, 7.5, 10, 15, or 20 mm). We used the 6D skull tracking method and full beam path set. CyberKnife has two beam placement methods: an isocentric technique, where the beam center is focused on the center of the target, and a non-isocentric technique, where each beam center is placed at the edge of the target without focusing on a single point. In this study, we used an isocentric technique to study simple conditions. A sequential algorithm is an optimization algorithm for the Precision treatment planning system that performs stepwise optimization by prioritizing multiple clinical targets, such as target dose coverage and spare organs at risk [24]. In this study, sequential algorithms were used. Beam alignment,

including monitor units (MUs), beam numbers, and beam directions, was optimized to align 70% of the maximum dose line to the GTV perimeter. A ray-tracing algorithm was used for dose calculation under high-resolution conditions (calculation voxel size = 0.5 × 0.5 × 0.5 mm).

The guidelines of the Radiation Therapy Oncology Group (RTOG) protocol 90-05 recommended adjusting the prescribed SRS dose for metastatic brain tumors according to tumor size [3]. Chang et al. used doses of 20–24 Gy for tumors < 20 mm in diameter following a dosage scheme established by the RTOG protocol 90-05 [25]. In this study, a dose of 20 Gy per fraction was prescribed for 95% of the GTV, and the prescription isodose line (IDL) was set to 70% of the maximum dose. These plans were created for each GTV and defined as reference plans (Fig. 1). Furthermore, error plans were created including intentionally generated target positioning errors (TPEs) relative to the reference plan to verify the target positioning accuracy. The precision treatment planning system allows shifting the beam incident points in steps of 0.01 mm, independent of voxel size. The TPEs were simulated by deliberately shifting the beam center from the GTV center in three dimensions with respect to the reference plan. TPEs were generated by shifting the beam center by the same magnitude in the x-axis (left/right direction), y-axis (anterior/superior direction), and z-axis (superior/inferior direction), and the coordinates of the beam center for the reference plan and plan involving TPE are represented by (x, y, z) and (x', y', z'), TPE is defined as the linear distance between the two centers and calculated by the following equation [21]:

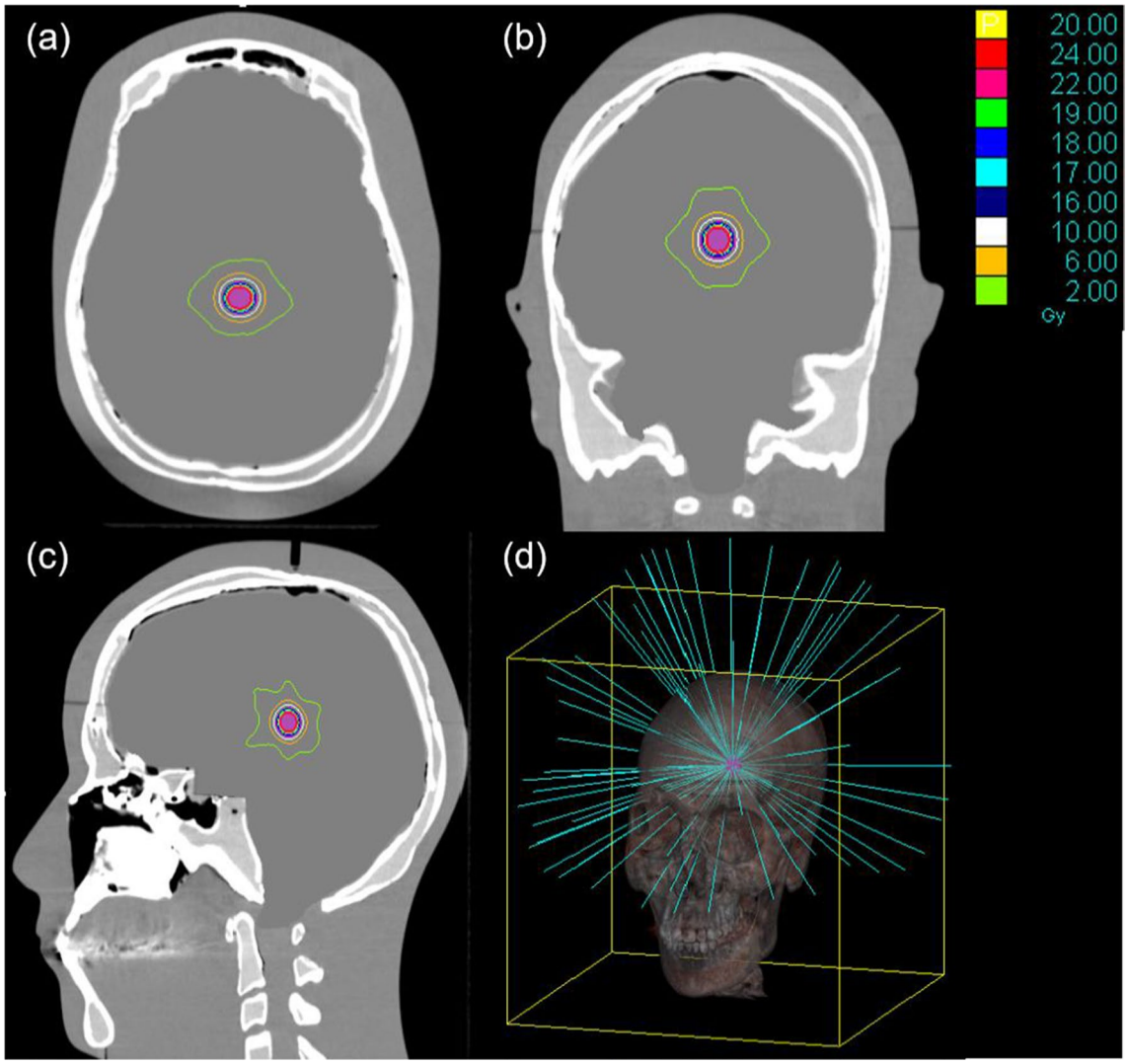

Fig. 1 Dose distributions for the reference plan at the gross tumor volume (GTV) with a 10-mm diameter (φ10-mm GTV): **a** axial, **b** coronal, and **c** sagittal views. **d** 3D view of the head phantom showing beam alignment for the reference plan at φ10-mm GTV. The magenta region represents the φ10-mm GTV

$$\mathrm{TPE} = \sqrt{(x' - x)^2 + (y' - y)^2 + (z' - z)^2}, \quad (1)$$

where $x' - x$, $y' - y$, and $z' - z$ are the shift distances along the x-, y-, and z-axes, respectively. In this study, shifts of the same magnitude were performed in each axis ($x' - x = y' - y = z' - z$) to generate TPE of 0.1 mm, 0.3 mm, 0.5 mm, 0.7 mm, 1.0 mm, 1.5 mm, and 2.0 mm. The dose distributions for all plans involving TPE were calculated with the same beam alignment as that used for the reference plan. Figure 2 shows the dose distributions for the reference plan and the plan involving a TPE of 2 mm at the φ10-mm GTV.

2.1 Evaluation index

We used a dose-volume histogram (DVH) to evaluate dose coverage and the values of D_{98} (dose covering 98% of the volume) and V_{20} (volume receiving ≥ 20 Gy) at each GTV. Dose conformity was analyzed using the conformity index (CI) [26], which was calculated using the following equation:

$$\mathrm{CI} = \frac{\mathrm{TV_{RI}}}{\mathrm{TV}} \times \frac{\mathrm{TV_{RI}}}{V_{\mathrm{RI}}}, \quad (2)$$

where TV, V_{RI}, and $\mathrm{TV_{RI}}$ are the target volume, the volume of the reference isodose, and the target volume covered by the reference isodose, respectively. In the present study, the reference isodose was defined as a 100% (20 Gy) isodose.

In the present study, we used an equivalent uniform dose (EUD)-based TCP model [11, 12, 21]. The DVH at each GTV was converted into a generalized equivalent uniform dose (gEUD) [27]. gEUD is defined as the biologically equivalent dose that results in the same TCP value obtained using a nonuniform dose distribution for a uniformly irradiated tumor, and it was calculated using the following equation:

$$\mathrm{gEUD} = \left[\sum_{i=1} v_i \cdot D_i^a\right]^{\frac{1}{a}}, \quad (3)$$

where v_i is unitless, represents the ith partial volume receiving dose D_i in Gy, and a represents a structure-specific unitless volume effect parameter that is negative for tumors [28, 29]. The value of "a" varies depending on the primary site and radiosensitivity of the tumor, making it difficult to define a single value for the evaluation of metastatic brain tumors [30–35]. In this study, two scenarios, "$a = -10$" and "$a = -5$," were investigated to assess their value within a reasonable range. These values were used in a study of treatment planning for non-small cell lung cancer (NSCLC) prone to brain metastasis [30–33, 36].

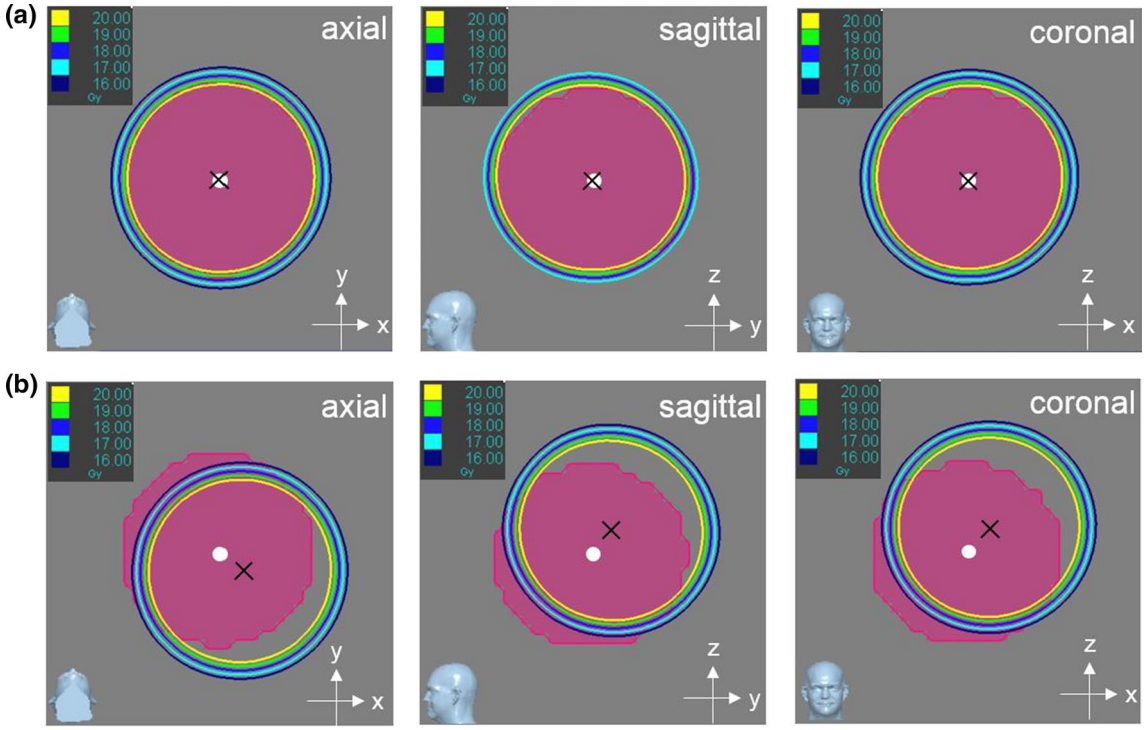

Fig. 2 Axial, sagittal, and coronal views (from left to right) showing the dose distributions for **a** the reference plan and **b** a plan involving a target positioning error (TPE) of 2 mm at the gross tumor volume (GTV) with a 10-mm diameter (φ10-mm GTV). The magenta, white, and black crosses represents the φ10-mm GTV, center of the GTV, and beam center, respectively

The biological effectiveness dose (BED) was evaluated based on the gEUD. In general, BED uses a linear-quadratic model to describe the responses to ionizing radiation at doses ≤ 18 Gy. However, the relationship between survival and dose approximates a linear relationship in the high-dose range [37–39]. Joiner proposed a linear-quadratic-cubic (LQC) model that adjusted for the linear response in the high-dose range [40]; in the present study, the LQC was used to calculate the BED using the following equation:

$$\mathrm{BED} = \mathrm{nd}\left[1 + \frac{d}{(\alpha/\beta)} - \frac{d^2}{(\alpha/\gamma)}\right], \tag{4}$$

$$\gamma = \frac{\beta}{3D_1}, \tag{5}$$

where n represents the number of dose fractions, and d represents the dose per fraction [40]. We used $\alpha/\beta = 12$ Gy to calculate BED_{12}, which reflects the fraction of surviving patients with brain metastases [41]. The value of D_1 represents the dose at which the survival curve straightens. The D_1 dose for brain metastases was set to 18 Gy to calculate the γ coefficient [40]. BED_{12} was calculated by converting the value of d into gEUD using Eq. (3) and then incorporating it along with the values of the above-mentioned parameters into Eq. (4):

$$\mathrm{BED}_{12} = \mathrm{gEUD}\left[1 + \frac{\mathrm{gEUD}}{12} - \frac{\mathrm{gEUD}^2}{648}\right]. \tag{6}$$

The TCP was calculated using the following equation described by Zindler et al. [11]:

$$\mathrm{TCP} = \frac{\mathrm{TCP}_{\max}}{1 + \left(\frac{D_{50}}{\mathrm{BED}_{12}}\right)^{4\gamma_{50}}}, \tag{7}$$

where D_{50} is the BED_{12} at a local control rate of 50%, γ_{50} is the normalized slope at D_{50}, and $\mathrm{TCP}_{\max}$ is the asymptotic local control rate for large D. Wiggenraad et al. reported the relationship between the dose and local control rate for metastatic brain tumors in a systematic review, whereby all prescription doses were converted to BED_{12} to compare different treatment schemes [1]. Zindler et al. estimated each parameter in Eq. (7) by fitting a logistic dose–response model using maximum likelihood estimation [11] and the relationship between the BED_{12} and 12-month local control rate, as described in a study by Wiggenraad et al. We adopted the following values from a previous report [11]: $\mathrm{TCP}_{\max} = 86.86\%$, $D_{50} = 28.97$ Gy, and $\gamma_{50} = 1.41$.

We calculated the TCP reduction rate of the plan involving TCP relative to the reference plan, plotted a graph showing the relationship between the TPE and TCP reduction rate for each GTV, and calculated the TPEs corresponding to the TCP reduction rates of 3%, 5%, and 10% by interpolation or extrapolation.

To estimate NTCP, we used the following equation to describe the NTCP of brain edema or necrosis as a function of V_{14} in the brain [13]:

$$\mathrm{NTCP} = \frac{\exp\left(4\gamma_{50}\left(\frac{V_{14}}{V_{x50}} - 1\right)\right)}{1 + \exp\left(4\gamma_{50}\left(\frac{V_{14}}{V_{x50}} - 1\right)\right)}, \tag{8}$$

where V_{x50} is V_{14} at an NTCP of 50% and γ_{50} is the normalized slope at V_{x50}. Milano et al. estimated each parameter in Eq. (8) using data from patients who developed grade 1–3 edema or necrosis after undergoing CyberKnife SRS for brain metastases [13]. In the present study, we adapted the following values from their report [13]: $V_{x50} = 45.8$ cc and $\gamma_{50} = 0.88$.

The gEUD, BED, TCP, and NTCP were calculated using MATLAB version 2020a (MathWorks, Natick, MA, USA).

In addition, we investigated the margin required to maintain the TCP of the GTV because TPE may have a significant impact on the TCP reduction rate at a GTV-PTV margin of 0 mm. We calculated the target diameter corresponding to each threshold value of the TCP reduction rate (3%, 5%, and 10%) for each TPE based on the relationship between the TCP reduction rate and GTV diameter for each TPE. In this study, we defined the TCP-based additional margin as the size of the additional margin required for each GTV to meet each acceptable value of the TCP reduction rate, according to the following equation:

$$\text{TCP based additional margin} = \frac{\mathrm{Dia.}_{\text{TCP - covered}} - \mathrm{Dia.}_{\mathrm{GTV}}}{2}, \tag{9}$$

where $\mathrm{Dia.}_{\text{TCP - covered}}$ is the target diameter corresponding to each threshold value of the TCP reduction rate and $\mathrm{Dia.}_{\mathrm{GTV}}$ is the GTV diameter. In addition, the NTCP values when TCP-based additional margin was given for each GTV was calculated from the relationship between the GTV diameter and NTCP.

3 Results

The beam characteristics for each reference plan are listed in Table 1. The number of beams and total MUs for the isocentric technique were optimized to 45–70 beams and 3873–5959 MU, respectively.

The results of the DVH analysis for each GTV diameter for the reference plans and plans involving TPE are presented in Fig. 3. The GTV dose coverage dramatically decreased as the value of TPE increased, especially for small GTVs.

Table 1 Beam characteristics for each reference plan

GTV diameter (mm)	Collimator diameter [mm]	Beam numbers	Total MUs
5	5	58	5959
7.5	7.5	67	5123
10	10	70	4938
15	15	50	4010
20	20	45	3873

The DVH parameters, TCP and NTCP, are summarized in Table 2. In the reference plans for all GTV size, the values of D_{98}, V_{20}, CI, TCP, and NTCP were in the range of 19.4–19.6 Gy, 94.9–95.2%, 0.90–0.93, 80.8–83.3%, and 2.91–4.72%, respectively (Table 2). TCP was lower for a gEUD parameter "a" of − 10 than for − 5, and NTCP was higher for larger GTV diameters. In the plans involving TPE, the dose coverage and TCP of the GTV dramatically decreased as TPE increased. In the plans involving a TPE of 2 mm, the values of D_{98}, V_{20}, and CI decreased to 8.4 Gy, 34.2%, and 0.12, respectively, at the φ5-mm GTV, which is the minimum. Similarly, TCP with gEUD parameters "a" of − 5 and − 10 decreased to 19.5% and 7.2%, respectively. In

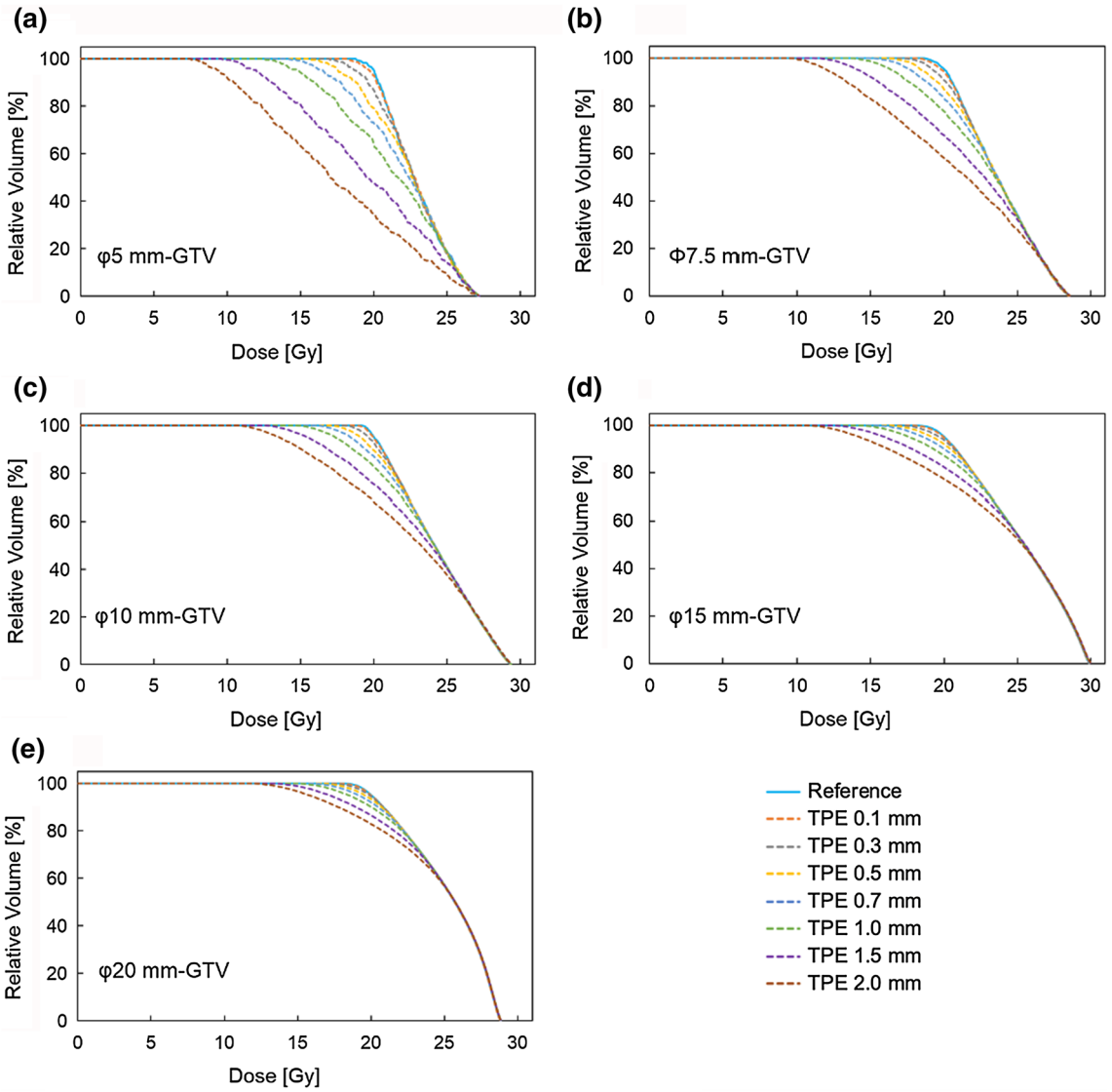

Fig. 3 Dose-volume histograms (DVHs) for each gross tumor volume (GTV) for the reference plans and plans involving TPE: **a** GTV with a 5-mm diameter (φ5-mm GTV), **b** GTV with a 7.5-mm diameter (φ7.5-mm GTV), **c** GTV with a 10-mm diameter (φ10-mm GTV), **d** GTV with a 15-mm diameter (φ15-mm GTV), and **e** GTV with a 20-mm diameter (φ20-mm GTV). The solid and dashed lines represent the DVHs for the reference plans and plans involving target positioning error (TPE), respectively

Table 2 DVH parameters, TCPs (parameter "*a*" in gEUD = − 5 and − 10), and NTCPs for the reference plans and plans involving TPE at each GTV

GTV diameter (mm)	Plan	GTV					Brain	
		D_{98} (Gy)	V_{20} (%)	CI	TCP (%)		V_{14} (cc)	NTCP (%)
					$a = -5$	a = − 10		
5	Reference	19.5	95.1	0.90	81.4	80.8	0.14	2.91
	TPE 0.1 mm	19.0	92.8	0.86	81.3	80.6	0.14	2.91
	TPE 0.3 mm	18.0	86.5	0.75	80.7	79.6	0.14	2.91
	TPE 0.5 mm	16.8	79.0	0.62	79.6	77.4	0.14	2.91
	TPE 0.7 mm	15.5	72.4	0.52	77.6	73.4	0.14	2.91
	TPE 1.0 mm	13.6	62.9	0.40	72.3	62.9	0.14	2.91
	TPE 1.5 mm	10.8	47.3	0.22	50.9	30.7	0.14	2.91
	TPE 2.0 mm	8.4	34.2	0.12	19.5	7.2	0.14	2.91
7.5	Reference	19.5	95.2	0.91	82.2	81.5	0.46	2.98
	TPE 0.1 mm	19.2	94.2	0.90	82.2	81.4	0.46	2.98
	TPE 0.3 mm	18.6	90.5	0.82	81.9	80.8	0.46	2.98
	TPE 0.5 mm	17.7	86.6	0.73	81.4	79.8	0.46	2.98
	TPE 0.7 mm	16.7	82.6	0.66	80.6	78.0	0.46	2.98
	TPE 1.0 mm	15.3	77.4	0.58	78.6	73.5	0.46	2.98
	TPE 1.5 mm	12.9	67.2	0.44	71.3	57.4	0.46	2.98
	TPE 2.0 mm	10.9	57.5	0.33	55.3	32.1	0.46	2.98
10	Reference	19.6	94.9	0.92	82.6	81.8	1.01	3.10
	TPE 0.1 mm	19.5	94.4	0.91	82.6	81.8	1.01	3.10
	TPE 0.3 mm	19.0	92.6	0.87	82.5	81.5	1.01	3.10
	TPE 0.5 mm	18.2	89.4	0.82	82.2	80.8	1.01	3.10
	TPE 0.7 mm	17.4	86.8	0.77	81.7	79.8	1.01	3.10
	TPE 1.0 mm	16.2	82.5	0.69	80.6	77.2	1.01	3.10
	TPE 1.5 mm	14.2	75.1	0.56	76.9	68.2	1.01	3.10
	TPE 2.0 mm	12.2	67.8	0.46	68.9	50.6	1.01	3.10
15	Reference	19.4	95.0	0.93	83.3	82.3	2.73	3.52
	TPE 0.1 mm	19.2	94.7	0.92	83.2	82.2	2.73	3.52
	TPE 0.3 mm	18.7	93.6	0.90	83.1	81.9	2.73	3.52
	TPE 0.5 mm	18.0	91.9	0.87	82.9	81.3	2.73	3.52
	TPE 0.7 mm	17.3	89.8	0.83	82.6	80.3	2.73	3.52
	TPE 1.0 mm	16.2	87.0	0.78	81.8	78.1	2.73	3.52
	TPE 1.5 mm	14.4	82.1	0.69	79.3	70.6	2.73	3.52
	TPE 2.0 mm	12.7	77.2	0.61	74.3	56.4	2.73	3.52
20	Reference	19.4	95.0	0.93	83.3	82.4	6.70	4.72
	TPE 0.1 mm	19.3	94.8	0.93	83.3	82.4	6.70	4.72
	TPE 0.3 mm	19.0	94.3	0.92	83.2	82.2	6.70	4.72
	TPE 0.5 mm	18.4	93.2	0.90	83.1	81.8	6.71	4.72
	TPE 0.7 mm	17.9	91.9	0.87	82.9	81.2	6.71	4.72
	TPE 1.0 mm	17.0	89.9	0.83	82.5	79.9	6.70	4.72
	TPE 1.5 mm	15.6	86.4	0.77	81.3	76.0	6.71	4.72
	TPE 2.0 mm	14.1	82.7	0.71	79.0	68.8	6.71	4.72

DVH dose-volume histogram, *GTV* gross tumor volume, *CI* conformity index, *TCP* tumor control probability, *NTCP* normal tissue complication probability, *TPE* target positioning error

contrast, the NTCPs at all GTVs were comparable regardless of the TPE value.

The relationship between the TCP reduction rate at each GTV and TPE is shown in Fig. 4. For a TPE of 0.3 mm, the TCP reduction rates at all GTVs with gEUD parameters "*a*" of − 5 and − 10 were < 0.8% and < 1.5%, respectively. However, for a TPE of 2.0 mm, the TCP reduction rates at the φ5-mm GTV with gEUD parameters "*a*" of − 5 and − 10 were 76% and 91%, respectively. The TPEs corresponding to TCP reduction rates of 3%, 5%, and 10% for

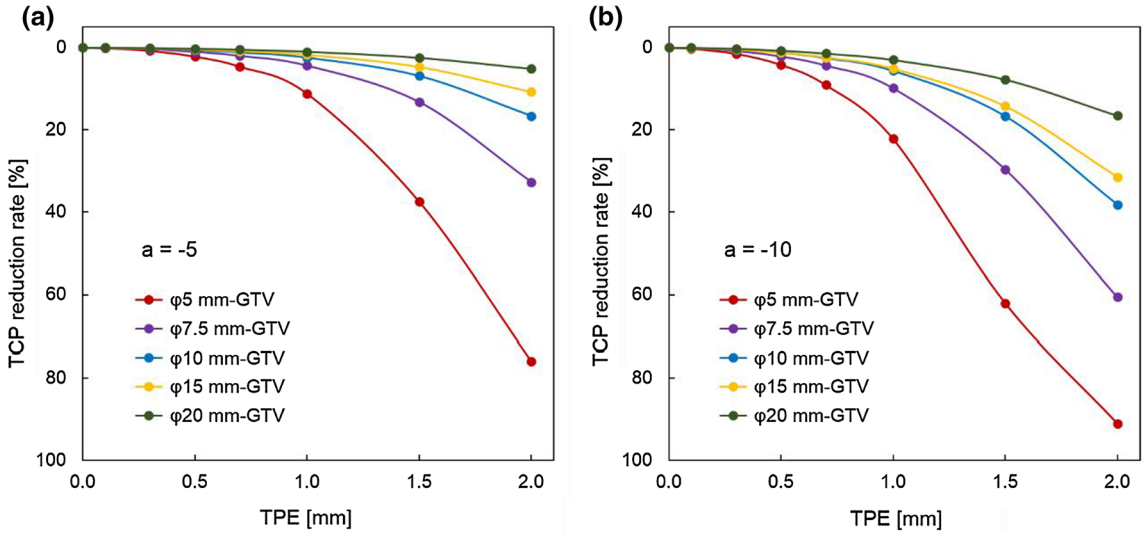

Fig. 4 Graph showing the relationship between the tumor control probability (TCP) reduction rate and the target positioning error (TPE) at each gross tumor volume (GTV) with generalized equivalent uniform dose (gEUD) parameters "*a*" of − 5 (**a**) and − 10 (**b**)

each GTV are summarized in Table 3. The smaller GTV was, the smaller the TPE corresponding to each threshold of the TCP reduction rate was; the TPE corresponding to 3% threshold of the TCP reduction rate at the *φ*5-mm GTV with gEUD parameters "*a*" of − 5 and − 10 were 0.57 mm and 0.41 mm, respectively (Table 3).

The relationship between the TCP reduction rate and GTV diameter for each TPE is shown in Fig. 5, and the TCP-based additional margins corresponding to TCP reduction rates of 3%, 5%, and 10% for each GTV diameter are summarized in Table 4. The TCP-based additional margins were larger for the increase in TPE, particularly for small GTVs. For a TPE of 1.0 mm and a TCP reduction rate of 3%, the TCP-based additional margins at the *φ*5-mm GTV with gEUD parameters "*a*" of − 5 and − 10 were 2.2 mm and 5.5 mm, respectively. The relationship between NTCP and TCP-based additional margins at each GTV is presented in Fig. 6. For a TCP-based additional margin of 2 mm, the increase in NTCP was < 1.2%, regardless of the GTV diameter.

4 Discussion

In the present study, we evaluated the effect of target positioning accuracy on dose distribution, TCP, and NTCP in SRS using CyberKnife for metastatic brain tumors of five different sizes. Our findings suggest that both the dose coverage and TCP at small GTVs decreased dramatically with an increase in TPE.

Previously, Guckenberger et al. reported an average reduction in CIs at a GTV of 10% due to a 1-mm setup error in LINAC-based SRS plans for metastatic brain tumors [17]. In the present study, we observed a 10% reduction in the CI corresponding to a TPE of 1 mm at the *φ*20-mm GTV in the present study. Our results are also similar to those of Winey et al., we found an approximately 61% reduction in the value

Table 3 TPE corresponding to TCP reduction rates of 3%, 5%, and 10% (parameter "*a*" in gEUD = − 5 and − 10) at each GTV

GTV diameter (mm)	TPE corresponding to the 3%, 5% and 10% of the TCP reduction rate (mm)					
	a = − 5			*a* = − 10		
	3%	5%	10%	3%	5%	10%
5	0.57	0.72	0.95	0.41	0.53	0.72
7.5	0.83	1.0	1.3	0.58	0.74	1.00
10	1.1	1.3	1.7	0.75	0.94	1.20
15	1.2	1.5	1.9	0.77	0.99	1.27
20	1.6	2.0	2.9	0.99	1.21	1.63

GTV gross tumor volume, *TPE* target positioning error, *TCP* tumor control probability

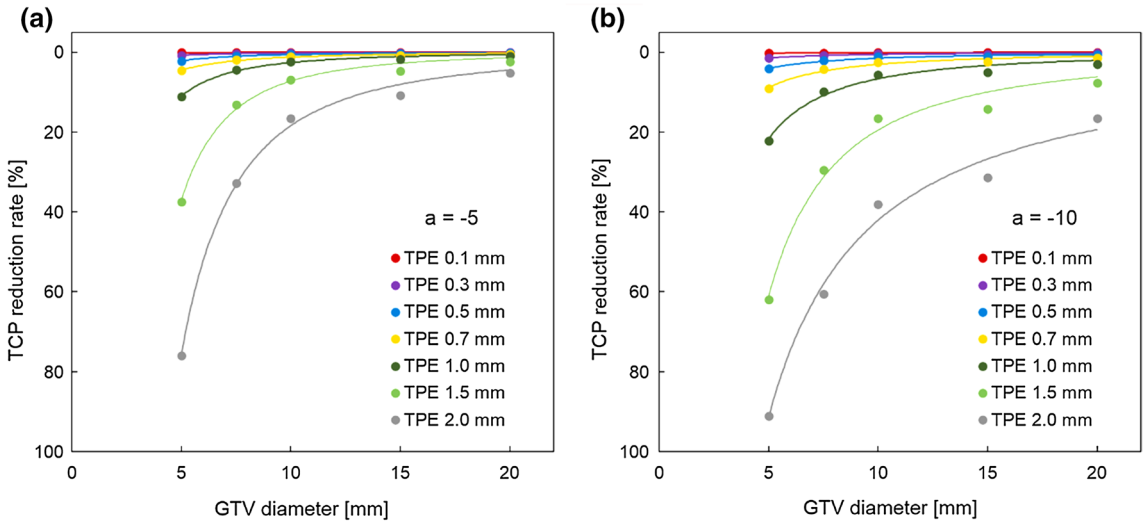

Fig. 5 Graph showing the relationship between tumor control probability (TCP) reduction rate and gross tumor volume (GTV) diameter for each target positioning error (TPE) with generalized equivalent uniform dose (gEUD) parameters "*a*" of − 5 (**a**) and − 10 (**b**)

of V_{20} for a TPE of 2 mm at a φ5-mm GTV [18]. In addition, the values of D_{98} and CI of the φ20-mm GTV for a TPE of 2 mm were reduced by approximately 57% (8.4 Gy) and 87% (0.12), respectively. These findings suggest that tumor size may reduce the target dose.

In the present study, the TCP for all GTVs in the reference plan was approximately 80% (80.8–83.3%). In contrast, the degree of TCP reduction varied markedly according to TPE and GTV diameters. The relationship between the dose and TCP follows a sigmoidal curve, which can be divided into a "shoulder" region with a gentle slope and a "linear" region with a steep slope [11]. For a GTV diameter of 5 mm, the same error caused a larger reduction in the TCP because the reduction occurs in the "linear" region due to a large reduction in the dose coverage.

The risk of brain necrosis is a major concern in SRS [13]. In the present study, the changes in NTCP for TPEs ≤ 2.0 mm were small for all GTVs (Table 2). In SRS for metastatic brain tumors using CyberKnife, V_{14} in the brain is associated with brain necrosis [13]. The risks of Grade 1–3 radiation brain necrosis for V_{14} of 5 cc, 10 cc, and 20 cc were estimated to be 4.1%, 6.0%, and 12.1%, respectively. [13]. In other words, NTCP changes significantly with a change in V_{14} of a few cc. However, because the change in V_{14} with TPE in this study was extremely small (within 0.01 cc), NTCP was comparable. This suggests that the effect of TPE on the risk of brain necrosis is relatively small, provided the dose constraint is satisfied in the reference plan.

We evaluated the TPE at each GTV corresponding to TCP reduction rates of 3%, 5%, and 10%. International Atomic Energy Agency Human Health Series No. 31 summarizes the accuracy and uncertainty of various radiotherapy processes [42]. Therein, the criterion for assessing the radiobiological impact of dose uncertainty was set as a 3% change in the TCP. From the results in Table 3, we believe that a TPE of 1 mm may be unacceptable.

We also observed that TCP-based additional margins increased with a decrease in target diameter and an increase in TPE. Nakano et al. evaluated the effect of setup errors in the single-isocenter technique on stereotactic radiosurgery for multiple brain metastases in a simulation study [19]. They found that coverage-based margins required to compensate for target dose reduction increased with a decrease in target diameter and an increase in six-degrees-of-freedom setup error [19]. Similar trends were also observed in the present study on SRS using CyberKnife, which also focused on the evaluation of radiobiological parameters such as TCP.

The values derived from the biological models largely depend on the selected model parameters. The use of reliable and appropriate parameters is essential for plan evaluation, as described in the AAPM-TG166 report [43]. In this study, we used the TCP and NTCP models based on the clinical outcomes of SRS/SRT for metastatic brain tumors [1, 11, 13]. However, we must pay attention to the selection of parameter "a" for the gEUD model. In general, negative values of "*a*" are used for tumors, and gEUD decreases with lower values of "*a*" [28, 31]. In NSCLC, which is prone to metastasis to the brain [36], "$a = -10$" for tumors is used to investigate radiotherapy planning [31, 32]. In addition, "$a = -5$" is associated with radioresponsive tumors and is used in treatment planning considerations for NSCLC [30, 33]. Similarly, "$a = -8$" and "$a = -7.2$" were used respectively for head and neck cancers and breast cancers, and the "a" used in this study is considered to be versatile even when brain metastases from these primary cancers are taken into account [34, 35]. In this study, TCP reduction by TPE was

Table 4 TCP-based additional margin corresponding to TCP reduction rates of 3%, 5%, and 10% (parameter "*a*" in gEUD = − 5 and − 10) at each GTV

GTV diameter (mm)	TPE (mm)	TCP-based additional margin corresponding to the 3%, 5% and 10% of the TCP reduction rate (mm)					
		a = − 5			*a* = − 10		
		3%	5%	10%	3%	5%	10%
5	0.1	0.0	0.0	0.0	0.0	0.0	0.0
	0.3	0.0	0.0	0.0	0.0	0.0	0.0
	0.5	0.0	0.0	0.0	0.6	0.0	0.0
	0.7	0.6	0.0	0.0	2.6	1.1	0.0
	1.0	2.2	1.2	0.1	5.5	3.4	1.4
	1.5	4.8	3.4	1.9	13.1	8.9	5.0
7.5	0.1	0.0	0.0	0.0	0.0	0.0	0.0
	0.3	0.0	0.0	0.0	0.0	0.0	0.0
	0.5	0.0	0.0	0.0	0.0	0.0	0.0
	0.7	0.0	0.0	0.0	1.3	0.0	0.0
	1.0	0.9	0.0	0.0	4.2	2.2	0.2
	1.5	3.5	2.1	0.6	11.8	7.7	3.7
10	0.1	0.0	0.0	0.0	0.0	0.0	0.0
	0.3	0.0	0.0	0.0	0.0	0.0	0.0
	0.5	0.0	0.0	0.0	0.0	0.0	0.0
	0.7	0.0	0.0	0.0	0.1	0.0	0.0
	1.0	0.0	0.0	0.0	3.0	0.9	0.0
	1.5	2.3	0.9	0.0	10.6	6.4	2.5
15	0.1	0.0	0.0	0.0	0.0	0.0	0.0
	0.3	0.0	0.0	0.0	0.0	0.0	0.0
	0.5	0.0	0.0	0.0	0.0	0.0	0.0
	0.7	0.0	0.0	0.0	0.0	0.0	0.0
	1.0	0.0	0.0	0.0	0.5	0.0	0.0
	1.5	0.0	0.0	0.0	8.1	3.9	0.0
20	0.1	0.0	0.0	0.0	0.0	0.0	0.0
	0.3	0.0	0.0	0.0	0.0	0.0	0.0
	0.5	0.0	0.0	0.0	0.0	0.0	0.0
	0.7	0.0	0.0	0.0	0.0	0.0	0.0
	1.0	0.0	0.0	0.0	0.0	0.0	0.0
	1.5	0.0	0.0	0.0	5.6	1.4	0.0

larger for "$a = -10$" than for "$a = -5$", indicating that the required target positioning accuracy varied with the value of "a". However, we suggest that the TPE of 1 mm might be unacceptable for both values of "*a*".

There are few reports on the overall positioning accuracy of CyberKnife, including treatment planning and irradiation. Pantelis et al. and Muacevic et al. reported overall positioning accuracy resulting from long-term quality control (QC) to be 0.40 ± 0.18 mm and 0.48 ± 0.22 mm, respectively [44, 45]. Based on our findings, the TCP reduction rate for a 0.3-mm error was < 1.5% for all GTVs. Consequently, the QC procedure for CyberKnife may require greater accuracy than that recommended by the AAPM TG135 report. Additionally, it is important to consider an appropriate margin to the GTV in terms of TCP and NTCP to consider the mechanical uncertainty. Based on the results of Table 4, a margin of 2.2 mm (gEUD parameters "*a*" of − 5) is required to maintain a TCP reduction rate within 3% for φ5-mm GTV under the condition with TPE of 1 mm. Figure 6 shows that the corresponding additional margin has little impact on the NTCP. These findings suggest that it may be possible to maintain a decrease in TCP and an increase in NTCP within clinically acceptable levels by adding an appropriate margin to the small GTV to consider the TPE.

In SRS/SRT for multiple brain metastases, it has been suggested that the target positioning accuracy is important for achieving a high local control rate [20]. It has also been reported that the D_{98} of the GTV is related to the local control rate of brain metastases [46]; therefore, it is clinically important to maintain the D_{98} of the GTV by meeting severe target positioning accuracy. Based on the results of this study, it is expected that the management of target

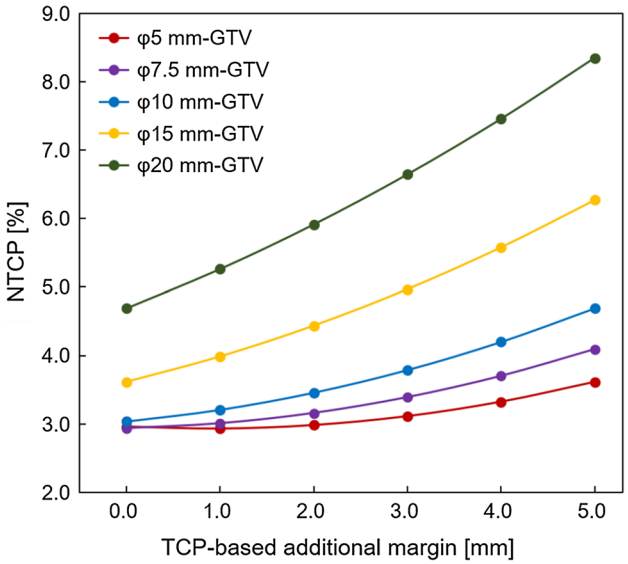

Fig. 6 Graph showing the relationship between normal tissue complication probability (NTCP) and tumor control probability (TCP)-based additional margin at each gross tumor volume (GTV)

positioning accuracy considering the tumor size will lead to improved clinical outcomes for metastatic brain tumors.

This study had some limitations. First, the present study did not consider variations in tumor shape and treatment plans. It is necessary to evaluate complex situations, including variations in GTV shape such as elliptical or irregular, variation in PTV margin, and variation in beam placement methods such as non-isocentric techniques in future work. Second, the prescribed IDL in this study was limited to 70%. In fact, the prescribed IDLs vary in SRS plans for metastatic brain tumors; previously, 80–90% and 50% IDLs were reported as the prescribed IDLs in LINAC and Gamma Knife-based SRS [1, 4]. However, differences in IDLs were not evaluated in this study. Previously, CyberKnife SRS plans have also been created with 55–92% IDLs as prescribed IDLs [8, 47]. In the present study, we applied commonly used 70% IDLs, bringing this evaluation to the safe side of 80–90% IDL; greater target positioning accuracy may be required for values of < 70% IDL. These limitations can be attributed to the fact that the present study was a phantom study. Therefore, further investigations based on clinical data from patients undergoing SRS should be conducted in the future.

5 Conclusions

TPE had a significant impact on the target dose coverage and TCP in SRS for metastatic brain tumors using CyberKnife, especially for small GTVs. However, TPE had a small impact on the NTCP. For a GTV diameter ≤ 20 mm, a geometric accuracy of < 1 mm is required to maintain the TCP reduction rate within a clinically acceptable level of 3%. These findings suggest the importance of additional margins according to mechanical uncertainty for small GTVs that are highly sensitive to TPE.

Acknowledgements This study was partially supported by Grants-in-Aid for Scientific Research–KAKENHI (Grant Nos. 19K17227, 20K16819, and 21K07722) from the Japanese Society for the Promotion of Science.

Declarations

Conflict of interest The authors declare no conflicts of interest.

Ethical approval This study did not involve any experiments using human participants or animals.

References

1. Wiggenraad R, Verbeek-de Kanter A, Kal HB, Taphoorn M, Vissers T, Struikmans H. Dose-effect relation in stereotactic radiotherapy for brain metastases. A systematic review. Radiother Oncol. 2011;98(3):292–7.
2. Aoyama H, Shirato H, Tago M, et al. Stereotactic radiosurgery plus whole-brain radiation therapy vs stereotactic radiosurgery alone for treatment of brain metastases: a randomized controlled trial. JAMA. 2006;295(21):2483–91.
3. Shaw E, Scott C, Souhami L, et al. Single dose radiosurgical treatment of recurrent previously irradiated primary brain tumors and brain metastases: final report of RTOG protocol 90-05. Int J Radiat Oncol Biol Phys. 2000;47(2):291–8.
4. Xu Q, Fan J, Grimm J, et al. The dosimetric impact of the prescription isodose line (IDL) on the quality of robotic stereotactic radiosurgery (SRS) plans. Med Phys. 2017;44(12):6159–65.
5. Treatment Centers. Accuray, Sunnyvale. https://www.accuray.com/treatment-centers/. Accessed 17 Dec 2021.
6. Kilby W, Dooley JR, Kuduvalli G, Sayeh S, Maurer CR. The CyberKnife® robotic radiosurgery system in 2010. Technol Cancer Res Treat. 2010;9(5):433–52.
7. Floriano A, Santa-Olalla I, Sanchez-Reyes A. Experience with the CyberKnife for intracranial stereotactic radiosurgery: analysis of dosimetry indices. Med Dosim. 2014;39(1):1–6.
8. Sio TT, Jang S, Lee SW, Curran B, Pyakuryal AP, Sternick ES. Comparing gamma knife and cyberknife in patients with brain metastases. J Appl Clin Med Phys. 2014;15(1):4095.
9. Han EY, Wang H, Luo D, Li J, Wang X. Dosimetric comparison of fractionated radiosurgery plans using frameless Gamma Knife ICON and CyberKnife systems with linear accelerator-based radiosurgery plans for multiple large brain metastases. J Neurosurg. 2019;132(5):1473–9.
10. Zhang S, Yang R, Wang X. Dosimetric quality and delivery efficiency of robotic radiosurgery for brain metastases: comparison with C-arm linear accelerator based plans. J Appl Clin Med Phys. 2019;20(11):104–10.
11. Zindler JD, Schiffelers J, Lambin P, Hoffmann AL. Improved effectiveness of stereotactic radiosurgery in large brain metastases by individualized isotoxic dose prescription: an in silico study. Strahlenther Onkol. 2018;194(6):560–9.

12. Wang H, Cooper BT, Schiff P, et al. Dosimetric assessment of tumor control probability in intensity and volumetric modulated radiotherapy plans. Br J Radiol. 2019;92(1094):20180471.
13. Milano MT, Grimm J, Niemierko A, et al. Single- and multifraction stereotactic radiosurgery dose/volume tolerances of the brain. Int J Radiat Oncol Biol Phys. 2020;3016(20):34101–8 (**in press**).
14. ICRU (International Commission on Radiation Units & Measurements). ICRU. Prescribing, recording, and reporting of stereotactic treatments with small photon beams. 2014.
15. Halvorsen PH, Cirino E, Das IJ, et al. AAPM-RSS medical physics practice guideline 9.a. for SRS-SBRT. J Appl Clin Med Phys. 2017;18(5):10–21.
16. Dieterich S, Cavedon C, Chuang CF, et al. Report of AAPM TG 135: quality assurance for robotic radiosurgery. Med Phys. 2011;38(6):2914–36.
17. Guckenberger M, Roesch J, Baier K, Sweeney RA, Flentje M. Dosimetric consequences of translational and rotational errors in frame-less image-guided radiosurgery. Radiat Oncol. 2012;7:63.
18. Winey B, Bussiere M. Geometric and dosimetric uncertainties in intracranial stereotatctic treatments for multiple nonisocentric lesions. J Appl Clin Med Phys. 2014;15(3):122–32.
19. Nakano H, Tanabe S, Utsunomiya S, et al. Effect of setup error in the single-isocenter technique on stereotactic radiosurgery for multiple brain metastases. J Appl Clin Med Phys. 2020;21(12):155–65.
20. Kraft J, van Timmeren JE, Mayinger M, et al. Distance to isocenter is not associated with an increased risk for local failure in LINAC-based single-isocenter SRS or SRT for multiple brain metastases. Radiother Oncol. 2021;159:168–75.
21. Nakano H, Tanabe S, Sasamoto R, et al. Radiobiological evaluation considering setup error on single-isocenter irradiation in stereotactic radiosurgery. J Appl Clin Med Phys. 2021;22(7):266–75.
22. Jhaveri J, Chowdhary M, Zhang X, et al. Does size matter? Investigating the optimal planning target volume margin for postoperative stereotactic radiosurgery to resected brain metastases. J Neurol Surg. 2018;130(3):797–803.
23. Eaton DJ, Lee J, Paddick I. Stereotactic radiosurgery for multiple brain metastases: results of multicenter benchmark planning studies. Pract Radiat Oncol. 2018;8(4):e212–20.
24. Schlaefer A, Schweikard A. Stepwise multi-criteria optimization for robotic radiosurgery. Med Phys. 2008;35(5):2094–103.
25. Chang EL, Selek U, Hassenbusch SJ III, et al. Outcome variation among "radioresistant" brain metastases treated with stereotactic radiosurgery. Neurosurgery. 2005;56(5):936–45 (**discussion 936**).
26. Paddick I, Lippitz B. A simple dose gradient measurement tool to complement the conformity index. J Neurol Surg. 2006;105(suppl):194–201.
27. Niemierko A. A generalized concept of equivalent uniform dose (EUD). Med Phys. 1999;26:1100.
28. Wu Q, Mohan R, Niemierko A, Schmidt-Ullrich R. Optimization of intensity-modulated radiotherapy plans based on the equivalent uniform dose. Int J Radiat Oncol Biol Phys. 2002;52(1):224–35.
29. Gay HA, Niemierko A. A free program for calculating EUD-based NTCP and TCP in external beam radiotherapy. Phys Med. 2007;23(3–4):115–25.
30. Chapet O, Thomas E, Kessler ML, Fraass BA, Ten Haken RK. Esophagus sparing with IMRT in lung tumor irradiation: an EUD-based optimization technique. Int J Radiat Oncol Biol Phys. 2005;63(1):179–87.
31. Chaikh A, Balosso J. The use of TCP based EUD to rank and compare lung radiotherapy plans: in-silico study to evaluate the correlation between TCP with physical quality indices. Transl Lung Cancer Res. 2017;6(3):366–72.
32. Chaikh A, Docquière N, Bondiau PY, Balosso J. Impact of dose calculation models on radiotherapy outcomes and quality adjusted life years for lung cancer treatment: do we need to measure radiotherapy outcomes to tune the radiobiological parameters of a normal tissue complication probability model? Transl Lung Cancer Res. 2016;5(6):673–80.
33. Zhao L, Chen M, Ten Haken R, et al. Three-dimensional conformal radiation may deliver considerable dose of incidental nodal irradiation in patients with early stage node-negative non-small cell lung cancer when the tumor is large and centrally located. Radiother Oncol. 2007;82(2):153–9.
34. Thieke C, Bortfeld T, Niemierko A, Nill S. From physical dose constraints to equivalent uniform dose constraints in inverse radiotherapy planning. Med Phys. 2003;30(9):2332–9.
35. Horton JK, Halle JS, Chang SX, Sartor CI. Comparison of three concomitant boost techniques for early-stage breast cancer. Int J Radiat Oncol Biol Phys. 2006;64(1):168–75.
36. Redmond KJ, Gui C, Benedict S, et al. Tumor control probability of radiosurgery and fractionated stereotactic radiosurgery for brain metastases. Int J Radiat Oncol Biol Phys. 2021;110(1):53–67.
37. Barendsen GW. Dose fractionation, dose rate and iso-effect relationships for normal tissue responses. Int J Radiat Oncol Biol Phys. 1982;8(11):1981–97.
38. Thames HD Jr, Withers HR, Peters LJ, Fletcher GH. Changes in early and late radiation responses with altered dose fractionation: implications for dose-survival relationships. Int J Radiat Oncol Biol Phys. 1982;8(2):219–26.
39. Brenner DJ. The linear-quadratic model is an appropriate methodology for determining isoeffective doses at large doses per fraction. Semin Radiat Oncol. 2008;18(4):234–9.
40. Joiner M. Quantifying cell kill and survival. In: Joiner M, van der Kogel A, editors. Basic clinical radiobiology. London: Hodder Arnold; 2009.
41. Yuan J, Wang JZ, Lo S, et al. Hypofractionation regimens for stereotactic radiotherapy for large brain tumors. Int J Radiat Oncol Biol Phys. 2008;72(2):390–7.
42. International Atomic Energy Agency (IAEA). Accuracy Requirements and Uncertainties in Radiotherapy. Human Health Series No. 31. Vienna: International Atomic Energy Agency; 2016.
43. Allen Li X, Alber M, Deasy JO, et al. The use and QA of biologically related models for treatment planning: short report of the TG-166 of the therapy physics committee of the AAPM. Med Phys. 2012;39(3):1386–409.
44. Pantelis E, Moutsatsos A, Antypas C, et al. On the total system error of a robotic radiosurgery system: phantom measurements, clinical evaluation and long-term analysis. Phys Med Biol. 2018;63(16): 165015.
45. Muacevic A, Kufeld M, Wowra B, Kreth FW, Tonn JC. Feasibility, safety, and outcome of frameless image-guided robotic radiosurgery for brain metastases. J Neurooncol. 2010;97(2):267–74.
46. Dupic G, Brun L, Molnar I, et al. Significant correlation between gross tumor volume (GTV) D98% and local control in multifraction stereotactic radiotherapy (MF-SRT) for unresected brain metastases. Radiother Oncol. 2021;154:260–8.
47. Dimitriadis A, Kirkby KJ, Nisbet A, Clark CH. Current status of cranial stereotactic radiosurgery in the UK. Br J Radiol. 2016;89(1058):20150452.